

Distributed Extended Object Tracking Information Filter Over Sensor Networks

Zhifei Li^{a,b,*}, Yan Liang^c, Linfeng Xu^c, Shuli Ma^a

^a*School of Space Information, Space Engineering University, Beijing 101400, China*

^b*College of Electronic Engineering, National University of Defense Technology, Hefei 230037, China*

^c*Laboratory of Information Fusion Technology, School of Automation, Northwestern Polytechnical University, Xi'an 710072, China*

Abstract

Motivated by the two common limitations on current distributed extended object tracking systems, i.e., an object is observable by each node, and its extent is modeled as an ellipse, this paper considers a multiplicative error model (MEM) to design the distributed information filter (IF) over a realistic network. The MEM reduces the extent of perpendicular axis-symmetric objects into a 3-D vector, which causes MEM being a nonlinear and state-coupled model with multiplicative noise. To meet the requirement in IF that the state-space model is a linear model with additive noise, we derive two separate pseudo-linearized models by using the first-order Taylor series expansion. The separation is merely in form, and the cross-correlation between states is preserved as parameters in each other's model. Thus, the joint estimation is transferred into an iterative operation of two linear filters. The two models is then applied to propose a centralized IF, where the measurements are converted into a summation of innovation parts. Later, under a sensor network with the communication nodes and sensor nodes, we present two distributed IFs based on the consensus on information and consensus on measurement schemes, respectively. Simulations indicate the performance of the proposed filters w.r.t accuracy, convergence, and consistency.

Keywords: Distributed consensus estimate, wireless sensor networks, sequential processing, extended object tracking

1. Introduction

Due to advances in sensor technology, the original belief that a sensor device's resolution is lower than the spatial extent of an object has become obsolete [1, 2]. In such a scenario, a single sensor may resolve multiple measurements from different scattering source on the object during a detection process. This causes a so-called extended object tracking (EOT) problem that estimate kinematic state and extent parameters simultaneously [3].

The past two decades have witnessed several approaches on how to model the extent, such as rectangle [4], ellipse [5, 6], axis-symmetric shapes modeled via multiplicative error model (MEM) [7, 8], or arbitrary shapes, modeled via random hyper-surface model (RHM) [9], Gaussian process (GP) [10–12], splines [13], or level-set RHM [14].

The range of the surveillance area and tracking performance will be increased over a sensor network containing multiple nodes, particularly if the nodes have narrow field-of-view and limited sensing distance [15–17]. Recently, G. Vivone et al. proposed a centralized EOT filter, where the fusion center gathered all data from entire network to yield current and future state estimate [18, 19]. The centralized tracking system

*Corresponding author

Email addresses: lee@seu.email.cn, lizhifei17@nudt.edu.cn (Zhifei Li), liangyan@nwpu.edu.cn (Yan Liang), xulinf@gmail.com (Linfeng Xu), shulima63@163.com (Shuli Ma)

provides an optimal estimate, but it faces the issue of data congestion, especially when the size of network is large. More importantly, the fusion service will be suspended or even denied if the fusion center is failed or suffers from network attacks.

In contrast to the centralized system, the distributed filter discards the fusion center, so it is more flexible and robust to the node and/or communication link failures. Due to the merits, the distributed tracking system has been widely used in many scenarios, such as surveillance, environment monitoring, and cyberspace situation awareness. To exchange sensor-based estimates among neighboring nodes, a distributed EOT filter was given by minimizing the weighted Kullback-Leibler divergence in [20]. To accomplish asynchronous data fusion between nodes, a distributed EOT particle filter was developed in [21], where the Geometric mean density (GMD) fusion rule was adopted to fuse the compressed Gaussian mixture approximations of local posterior probability density functions. In [22], a distributed variational Bayesian filter was derived for jointly estimating the EO states and measurement noise covariance. Therein, the alternating direction method of multipliers (ADMM) technique was used to achieve the constrained consensus estimate. The consensus strategy is referred to as *Consensus on Estimate* (CE) [23, 24].

The aforementioned distributed filters over sensor networks have two main limitations. First, these filters rely on the RM model that describes the extent of EO as an ellipse. The model is a simple, effective, and universal framework, while it is not suitable for different types of objects. For example, the extent of a bus should be modeled as a rectangle rather than an ellipse. Moreover, the model involves a special structure (i.e., the process noise covariance is related to the object's extent) to ensure a recursive operation, so that other interested kinematic states, such as the yaw rate, cannot be easily merged into the state vector. Second, these filters assume that an EO is visible to all nodes regardless of the scan time. However, in a practical sensor network, each node only views an EO at some specific time, even though the full set of nodes view the object at any time. To the best of our knowledge, no literature explores others models (e.g., GP model, MEM model) to present a distributed EOT filter over a realistic sensor network.

In this paper, we endeavor to design a distributed extended object tracking filter over a sensor network consisting of communication nodes and sensor nodes. The network architecture is regarded as a general case of a realistic network, and the communication nodes are supposed to be the nodes that cannot detect an object. The object extent is described by the state-coupled MEM model proposed in [8] that partitions the extent into a 3-D vector including semi-axes and orientation. Based on the MEM model, we derive two distributed information filters to simultaneously yield a consensus estimate on the extent and kinematic state. The main contributions are as follows.

1. We establish two separate pseudo-linearized measurement models with only additive noise by using the first-order Taylor series expansion. The two models are consistent with the first and second moment information of the original MEM model.
2. This paper presents a compact centralized information filter based on the two models, where the massive measurements are converted into a summation form of innovation parts. The centralized filter serves as a benchmark to determine the performance of the corresponding distributed filter.
3. The two models are combined into *Consensus on Information* (CI) and *Consensus on Measurement* (CM) schemes, respectively. Following this, we give two types of distributed information filters by using a so-called arithmetic average fusion rule to yield the consensus estimates on both the extent and kinematic state.

The rest of the paper is organized as follows. Section 2 gives a brief problem formulation. Section 3 presents two separate measurement models. Section 4 gives a centralized filter and Section 5 presents two corresponding distributed filters. The proposed filters are demonstrated by numerical examples in Section 6. Section 7 concludes this paper.

Notation: For clarity, we use italics to denote scalar quantities and boldface for vectors and matrices. We use “:=” to define a quantity and $(\cdot)^T$ denotes the transpose of a matrix /vector. The n -th dimensional identity matrix is denoted by \mathbf{I}_n . Operation $\text{col}(\mathbf{A}_i)_{i \in \mathcal{N}}$, where \mathcal{N} is a finite set, denotes stacking \mathbf{A}_i on top of each other to form a column matrix.

2. Problem Formulation

Here, we consider the MEM model proposed in [8] to achieve the centralized and distributed information filters over a sensor network [25]. The network consisting of two types of nodes is deployed over a geographic region. Therein, the *Communication* nodes process local measurements as well as communicate with neighboring nodes, while *Sensor* nodes also have sensing capabilities. The network is served as a general case of a realistic network architecture, where the communication nodes represent those nodes that cannot obtain measurements due to their narrow field-of-view or limited sensing distance. The network is denoted by triplet $(\mathcal{S}, \mathcal{C}, \mathcal{A})$, where \mathcal{S} is the set of sensor nodes, \mathcal{C} is the set of communication nodes, $\mathcal{N} = \mathcal{S} \cup \mathcal{C}$, $\mathcal{A} \subseteq \mathcal{N} \times \mathcal{N}$ is the set of edges such that $(s, j) \in \mathcal{A}$ if node s can communicate with j . For each node $s \in \mathcal{N}$, \mathcal{N}^s denotes the set of its neighboring nodes (including s itself), i.e., $\mathcal{N}^s := \{j : (j, s) \in \mathcal{A}\}$, and let $\mathcal{N}^s \setminus \{s\}$ be the set of its neighboring nodes (excluding s itself). The accumulated sensor data of node $s \in \mathcal{S}$ at time k is denoted as $\mathcal{Y}_{k,s} = \{\mathbf{y}_{k,s}^i\}_{i=1}^{n_{k,s}}$, and the accumulated data from all sensor nodes is denoted as $\mathcal{Y}_k = \{\mathcal{Y}_{k,s}\}_{s \in \mathcal{S}}$.

Next, we first review the MEM model.

1. State Parameterization

The kinematic state \mathbf{x}_k of an EO at time k

$$\mathbf{x}_k = [\mathbf{m}_k^\top, \dot{\mathbf{m}}_k^\top, \dots]^\top \quad (1)$$

includes the position \mathbf{m}_k , velocity $\dot{\mathbf{m}}_k$, and interested quantities such as acceleration. The extent at time k

$$\mathbf{p}_k = [\alpha_k, l_{k,1}, l_{k,2}]^\top \in \mathbb{R}^3 \quad (2)$$

includes the orientation α_k , which denotes the counterclockwise rotation angle along the x -axis, and the semi-axes lengths $l_{k,1}$ and $l_{k,2}$.

2. Measurement Model

At time k , the i -th measurement \mathbf{y}^i on sensor node $s \in \mathcal{S}$ is modeled as

$$\mathbf{y}_{k,s}^i = \mathbf{H}\mathbf{x}_k + \underbrace{\begin{bmatrix} \cos \alpha_k & -\sin \alpha_k \\ \sin \alpha_k & \cos \alpha_k \end{bmatrix} \begin{bmatrix} l_{1,k} & 0 \\ 0 & l_{2,k} \end{bmatrix}}_{:=\mathbf{S}_k} \underbrace{\begin{bmatrix} h_{k,1}^i \\ h_{k,2}^i \end{bmatrix}}_{:=\mathbf{h}_{k,s}^i} + \mathbf{v}_{k,s}^i \quad (3)$$

where $\mathbf{H} = [\mathbf{I}_2 \ \mathbf{0}]$ is the measurement matrix, \mathbf{S}_k compacts the orientation and size for the considered EO, multiplicative noise $\mathbf{h}_{k,s}^i$ guarantees that any scattering source \mathbf{z}_k lies on the boundary or interior of an object (see Fig. 1), and $\mathbf{v}_{k,s}^i, \mathbf{v}_{k,j}^i, \dots$ are uncorrelated zero-mean Gaussian noises with covariances $\mathbf{C}_s^v \delta_{sj}$ if $s = j$, $\delta_{sj} = 1$, and $\delta_{sj} = 0$, otherwise.

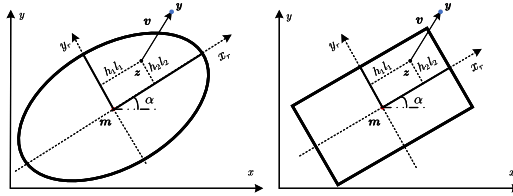


Figure 1: Illustration of the measurement model. The time index k , measurement index $[i]$, and sensor node index s are omitted in the figure. The centroid position of the object is $\mathbf{m} = [m_1, m_2]^\top$, and its extent is denoted as $\mathbf{p} = [\alpha, l_1, l_2]^\top$. By counterclockwise rotating an angle α (i.e., the orientation) along the x -axis, we get the reference coordinates x_r - y_r . The scattering source \mathbf{z} is determined by parameters \mathbf{p} , \mathbf{m} , and multiplicative noise $\mathbf{h} = [h_1, h_2]^\top$. The measurement \mathbf{y} is generated via the source \mathbf{z} plus a Gaussian measurement noise \mathbf{v} . The illustration gives an intuitive insight that the measurement model is feasible to describe the perpendicular axis-symmetric shapes, such as an ellipse or a rectangular.

3. Dynamic Models

The dynamic models for the kinematic state and extent are shown as follows, respectively

$$\mathbf{x}_{k+1} = \mathbf{F}_k^x \mathbf{x}_k + \mathbf{w}_k^x \quad (4)$$

$$\mathbf{p}_{k+1} = \mathbf{F}_k^p \mathbf{p}_k + \mathbf{w}_k^p \quad (5)$$

where \mathbf{F}_k^x and \mathbf{F}_k^p are state transition matrices, and \mathbf{w}_k^x and \mathbf{w}_k^p are zero-mean Gaussian process noises with covariances \mathbf{C}_w^x and \mathbf{C}_w^p , respectively. One can select the corresponding transition matrices according to the actual motion model and body structure, e.g., for a rigid object with nearly constant velocity,

$$\mathbf{F}_k^s = \begin{bmatrix} 1 & 0 & T & 0 \\ 0 & 1 & 0 & T \\ 0 & 0 & 1 & 0 \\ 0 & 0 & 0 & 1 \end{bmatrix}, \quad \mathbf{F}_k^p = \mathbf{I}_3$$

where T is the scan time.

This paper selects the MEM model rather than the RM model used in [22] mainly because it has the following merits: (1) it reduces the estimation of symmetric positive-definite matrix (i.e., the extent) to estimate 3-D vector \mathbf{p}_k , (2) in contrast to the RM model, the dynamic models (4) and (5) are treated independently, allowing for other kinematic states to be incorporated into the state vector, and (3) the uncertainty of the extent is determined by the semi-axes and orientation, not a degree of freedom scalar.

In spite of the state-space model is given, it is still challenging to directly use the model to provide a centralized or distributed filter. For the centralized filter, a main difficulty is how to handle the massive measurements from multiple nodes, which will be more intractable in the EOT scenario. In the considered network, the distributed filter encounters the difficulty: how to give a proper scheme to balance the estimates or measurements between the sensor nodes and communication nodes and simultaneously yield consensus estimates on both kinematic state and extent.

3. Separation of measurement model with coupled kinematics and extent

The paper introduces the information-matrix fusion (IMF) to address the aforementioned difficulties. The IMF originates from the information filter that recursively updates the information matrix (inverse of the error covariance) and information vector (information matrix multiply by the estimate) [26]. The IMF provides two main advantages: (1) in the centralized filter, the measurements from multiple nodes can be converted into a summation form, (2) in the distributed filter, the information vector (includes the error covariance) on each node is easily set to be different weight in the ultimate consensus estimate. However, the information filter requires a linear measurement model with only additive noise for each estimated state. It is shown that the measurement model (3) with multiplicative noise does not meet the requirement. Hence, the top priority is to construct two separate linear measurement models with only additive noise w.r.t \mathbf{x}_k and \mathbf{p}_k . Then, an interaction design within the related filters is necessary for a convergent output.

Assume that the measurements $\{\mathbf{y}_{k,s}^i\}_{i=1}^{n_{k,s}}$ at each sensor node $s \in \mathcal{S}$ are sequentially processed. Let $\hat{\mathbf{x}}_k^{[i-1]}$, $\hat{\mathbf{p}}_k^{[i-1]}$, $\mathbf{C}_k^{x[i-1]}$ and $\mathbf{C}_k^{p[i-1]}$ denote the estimates for the kinematics \mathbf{x}_k and extent \mathbf{p}_k plus corresponding covariances at the $[i-1]$ -th sequential operation. The node s processes $\mathbf{y}_{k,s}^i$ to obtain the updated estimates $\hat{\mathbf{x}}_k^{[i]}$, $\hat{\mathbf{p}}_k^{[i]}$, $\mathbf{C}_k^{x[i]}$ and $\mathbf{C}_k^{p[i]}$. Next, we focus on constructing two pseudo-linearized measurement models w.r.t \mathbf{x}_k and \mathbf{p}_k , respectively.

Proposition 1. The measurement model related to \mathbf{x}_k is

$$\mathbf{y}_{k,s}^i \approx \mathbf{H} \mathbf{x}_k + \mathbf{v}_{k,s}^{x[i]} \quad (6)$$

where $\mathbf{v}_{k,s}^{x[i]}$ is the equivalent noise about \mathbf{x}_k with $\mathbb{E}(\mathbf{v}_{k,s}^{x[i]}) = \mathbf{0}$ and $\text{Cov}(\mathbf{v}_{k,s}^{x[i]}) = \mathbf{R}_{k,s}^{x[i]} := \mathbf{C}^I + \mathbf{C}^{II} + \mathbf{C}_s^v$. The terms \mathbf{C}^I and \mathbf{C}^{II} are

$$\mathbf{C}^I = \hat{\mathbf{S}}_k^{[i-1]} \mathbf{C}^h \left(\hat{\mathbf{S}}_k^{[i-1]} \right)^\top \quad (7)$$

$$\underbrace{[\epsilon_{mn}]_{\mathbf{C}^{II}}} = \text{tr} \left\{ \mathbf{C}_k^{p[i-1]} \left(\hat{\mathbf{J}}_{n,k}^{[i-1]} \right)^\top \mathbf{C}^h \hat{\mathbf{J}}_{m,k}^{[i-1]} \right\} \quad (8)$$

for $m, n \in \{1, 2\}$. The quantities $\hat{\mathbf{J}}_{1,k}^{[i-1]}$ and $\hat{\mathbf{J}}_{2,k}^{[i-1]}$ are the Jacobian matrices of the first row $\mathbf{S}_{1,k}$ and second row $\mathbf{S}_{2,k}$ of \mathbf{S}_k around the $[i-1]$ -th extent estimate $\hat{\mathbf{p}}_k^{[i-1]}$, respectively.

PROOF OF PROPOSITION 1. Considering that the true extent \mathbf{p}_k is unknown in the shape matrix \mathbf{S}_k . Performing the first-order Taylor series expansion of term $\mathbf{S}_k \mathbf{h}_{k,s}^i$ in (3) around the $[i-1]$ -th extent estimate $\hat{\mathbf{p}}_k^{[i-1]}$ and keeping $\mathbf{h}_{k,s}^i$ as a random variable yields

$$\mathbf{S}_k \mathbf{h}_{k,s}^i \approx \underbrace{\hat{\mathbf{S}}_k^{[i-1]} \mathbf{h}_{k,s}^i}_{\text{I}} + \underbrace{\begin{bmatrix} \left(\mathbf{h}_{k,s}^i \right)^\top \hat{\mathbf{J}}_{1,k}^{[i-1]} \\ \left(\mathbf{h}_{k,s}^i \right)^\top \hat{\mathbf{J}}_{2,k}^{[i-1]} \end{bmatrix}}_{\text{II}} \left(\mathbf{p}_k - \hat{\mathbf{p}}_k^{[i-1]} \right). \quad (9)$$

Substituting (9) into (3), the residual covariance about $\mathbf{y}_{k,s}^{[i]}$ in (3) is calculated as

$$\mathbf{C}_{k,s}^{y[i]} = \mathbf{H} \mathbf{C}_k^{x[i-1]} \mathbf{H}^\top + \mathbf{C}^I + \mathbf{C}^{II} + \mathbf{C}_s^v, \quad (10)$$

and (3) is rewritten as (6). The proof is complete. \square

Note that the quantities \mathbf{C}^I and \mathbf{C}^{II} in (10) are treated as constant terms at the $[i]$ -th sequential operation since they are calculated based on the former estimate $\hat{\mathbf{p}}_k^{[i-1]}$.

As pointed out in [8, 27], a pseudo-measurement using 2-fold Kronecker product is required to update the extent. The i -th pseudo-measurement \mathbf{Y}_k^i is given as

$$\mathbf{Y}_{k,s}^i = \mathbf{F} \left(\left(\mathbf{y}_{k,s}^i - \mathbf{H} \hat{\mathbf{x}}_k^{[i-1]} \right) \otimes \left(\mathbf{y}_{k,s}^i - \mathbf{H} \hat{\mathbf{x}}_k^{[i-1]} \right) \right) \quad (11)$$

with

$$\mathbf{F} = \begin{bmatrix} 1 & 0 & 0 & 0 \\ 0 & 0 & 0 & 1 \\ 0 & 1 & 0 & 0 \end{bmatrix}. \quad (12)$$

Based on (11), the following proposition 2 gives the measurement model w.r.t the extent \mathbf{p}_k .

Proposition 2. The measurement model related to \mathbf{p}_k is

$$\mathbf{Y}_{k,s}^i \approx \hat{\mathbf{M}}_k^{[i-1]} \mathbf{p}_k + \mathbf{v}_{k,s}^{p[i]} \quad (13)$$

where $\mathbf{v}_{k,s}^{p[i]}$ is the equivalent noise about \mathbf{p}_k with

$$\begin{aligned} \mathbb{E}(\mathbf{v}_{k,s}^{p[i]}) &= \bar{\mathbf{v}}_{k,s}^{p[i]} = \mathbf{F} \text{vect} \left(\mathbf{C}_{k,s}^{y[i]} \right) - \hat{\mathbf{M}}_k^{[i-1]} \hat{\mathbf{p}}_k^{[i-1]}, \\ \text{Cov}(\mathbf{v}_{k,s}^{p[i]}) &= \mathbf{R}_{k,s}^{p[i]} := \mathbf{F} \left(\mathbf{C}_{k,s}^{y[i]} \otimes \mathbf{C}_{k,s}^{y[i]} \right) (\mathbf{F} + \tilde{\mathbf{F}})^\top \\ &\quad - \hat{\mathbf{M}}_k^{[i-1]} \mathbf{C}_k^{p[i-1]} \left(\hat{\mathbf{M}}_k^{[i-1]} \right)^\top, \end{aligned}$$

with

$$\tilde{\mathbf{F}} = \begin{bmatrix} 1 & 0 & 0 & 0 \\ 0 & 0 & 0 & 1 \\ 0 & 0 & 1 & 0 \end{bmatrix}, \quad (14)$$

and

$$\hat{\mathbf{M}}_k^{[i-1]} = \begin{bmatrix} 2\hat{\mathbf{S}}_{1,k}^{[i-1]} \mathbf{C}^h \hat{\mathbf{J}}_{1,k}^{[i-1]} \\ 2\hat{\mathbf{S}}_{2,k}^{[i-1]} \mathbf{C}^h \hat{\mathbf{J}}_{2,k}^{[i-1]} \\ \hat{\mathbf{S}}_{1,k}^{[i-1]} \mathbf{C}^h \hat{\mathbf{J}}_{2,k}^{[i-1]} + \hat{\mathbf{S}}_{2,k}^{[i-1]} \mathbf{C}^h \hat{\mathbf{J}}_{1,k}^{[i-1]} \end{bmatrix}. \quad (15)$$

PROOF OF PROPOSITION 2. see Appendix A. \square

Note that $\hat{\mathbf{M}}_k^{[i-1]}$ is the corresponding measurement matrix w.r.t \mathbf{p}_k , and it is treated as constant terms at the $[i]$ -th sequential operation.

Remark 1. • The models (6) and (13) are separate in form, but the cross-correlation about \mathbf{x}_k and \mathbf{p}_k is remained in each other's model. In this way, the joint estimation is merged into an iterative implementation of two linear filters.

- The models (6) and (13) only utilize the first-order Taylor series expansion in (9), omitting the higher-order terms. On the one hand, they avoid some complex calculations, such as the Hessian matrix. On the other hand, (13) only relies on the first-order expansion as a prerequisite, otherwise (13) cannot be derived.

4. Centralized Extended Object Tracking Filter

Intuitively, a sensor network increases the perception capability for an EO from different perspectives because a single node with limited local observability may cause the measurement missing in a specific field-of-view [22, 25]. Here, we derive a centralized EOT (CEOT) information filter by using the two models (6) and (13). Information filter updates, instead of the estimate $\hat{\mathbf{x}}_k^{[i]}(\hat{\mathbf{p}}_k^{[i]})$ and its error covariance $\mathbf{C}_k^{x[i]}(\mathbf{C}_k^{p[i]})$, the information matrix $\boldsymbol{\Omega}_k^{x[i]} := (\mathbf{C}_k^{x[i]})^{-1}$ and information vector $\hat{\mathbf{q}}_k^{x[i]} := (\mathbf{C}_k^{x[i]})^{-1} \hat{\mathbf{x}}_k^{[i]}$ [26].

In CEOT filter, the fusion center sequentially processes all measurements $\mathcal{Y}_k = \{\mathcal{Y}_{k,s}\}_{s \in \mathcal{S}}$ from all sensor nodes to obtain an estimate. Assume that there are n_k measurements, for clarity, on each sensor node $s \in \mathcal{S}$ at time k . Given the $[i-1]$ -th estimates $\hat{\mathbf{q}}_k^{x[i-1]}$, $\hat{\mathbf{q}}_k^{p[i-1]}$, $\boldsymbol{\Omega}_k^{x[i-1]}$ and $\boldsymbol{\Omega}_k^{p[i-1]}$, the center processes the measurement set $\{\mathbf{y}_{k,s}^i\}_{s \in \mathcal{S}}$ to give the $[i]$ -th estimates. Notice that the notation $(\cdot)_k^{[0]}$ is the corresponding predicted estimates at time k .

Define the central measurement, measurement matrix, and noise covariance related to the measurement set $\{\mathbf{y}_{k,s}^i\}_{s \in \mathcal{S}}$ as

$$\begin{cases} \mathbf{y}_{k,c}^i := \text{col}(\mathbf{y}_{k,1}^i, \mathbf{y}_{k,2}^i, \dots, \mathbf{y}_{k,|\mathcal{S}|}^i) \\ \mathbf{H}_c^{[i]} := [\mathbf{H}; \mathbf{H}; \dots; \mathbf{H}] \\ \mathbf{R}_{k,c}^{x[i]} := \text{diag}(\mathbf{R}_{k,1}^{x[i]}, \mathbf{R}_{k,2}^{x[i]}, \dots, \mathbf{R}_{k,|\mathcal{S}|}^{x[i]}) \end{cases} \quad (16)$$

where the subscript ‘‘c’’ denotes ‘‘central’’, and $|\mathcal{S}|$ is the cardinality of \mathcal{S} .

Define the central measurement, measurement matrix, and noise covariance related to the pseudo-measurement set $\{\tilde{\mathbf{Y}}_{k,s}^i\}_{s \in \mathcal{S}}$ as

$$\begin{cases} \tilde{\mathbf{Y}}_{k,s}^{[i]} := \mathbf{Y}_{k,s}^i - \mathbf{F}\text{vect}(\mathbf{C}_{k,s}^{y[i]}) + \hat{\mathbf{M}}_k^{[i-1]} \hat{\mathbf{p}}_k^{[i-1]} \\ \tilde{\mathbf{Y}}_{k,c}^{[i]} := \text{col}(\tilde{\mathbf{Y}}_{k,1}^{[i]}, \tilde{\mathbf{Y}}_{k,2}^{[i]}, \dots, \tilde{\mathbf{Y}}_{k,|\mathcal{S}|}^{[i]}) \\ \mathbf{M}_{k,c}^{[i]} := [\hat{\mathbf{M}}_k^{[i-1]}; \hat{\mathbf{M}}_k^{[i-1]}; \dots; \hat{\mathbf{M}}_k^{[i-1]}] \\ \mathbf{R}_{k,c}^{p[i]} = \text{diag}(\mathbf{R}_{k,1}^{p[i]}, \mathbf{R}_{k,2}^{p[i]}, \dots, \mathbf{R}_{k,|\mathcal{S}|}^{p[i]}) \end{cases}. \quad (17)$$

Introducing the noise information matrices $\mathbf{W}_w^x := (\mathbf{C}_w^x)^{-1}$, $\mathbf{W}_w^p := (\mathbf{C}_w^p)^{-1}$, $\mathbf{V}_{k,s}^{x[i]} := (\mathbf{R}_{k,s}^{x[i]})^{-1}$ and $\mathbf{V}_{k,s}^{p[i]} := (\mathbf{R}_{k,s}^{p[i]})^{-1}$, CEOT filter based on (16) and (17) consists of two steps:
(1) Measurement Update Step (Correction)

$$\hat{\mathbf{q}}_k^{x[i]} = \hat{\mathbf{q}}_k^{x[i-1]} + \sum_{s \in \mathcal{S}} \mathbf{H}^\top \mathbf{V}_{k,s}^{x[i]} \mathbf{y}_{k,s}^i \quad (18a)$$

$$\mathbf{\Omega}_k^{x[i]} = \mathbf{\Omega}_k^{x[i-1]} + \sum_{s \in \mathcal{S}} \mathbf{H}^\top \mathbf{V}_{k,s}^{x[i]} \mathbf{H}, \quad (18b)$$

$$\hat{\mathbf{q}}_k^{p[i]} = \hat{\mathbf{q}}_k^{p[i-1]} + \sum_{s \in \mathcal{S}} \left(\hat{\mathbf{M}}_k^{[i-1]} \right)^\top \mathbf{V}_{k,s}^{p[i]} \tilde{\mathbf{Y}}_{k,s}^{[i]} \quad (19a)$$

$$\mathbf{\Omega}_k^{p[i]} = \mathbf{\Omega}_k^{p[i-1]} + \sum_{s \in \mathcal{S}} \left(\hat{\mathbf{M}}_k^{[i-1]} \right)^\top \mathbf{V}_{k,s}^{p[i]} \hat{\mathbf{M}}_k^{[i-1]}. \quad (19b)$$

From (18) and (19), using the models (6) and (13) to construct an IMF form further reduces the computational cost, since they convert the measurements from the sensor nodes into a summation term of innovation parts (we refer $\mathbf{H}^\top \mathbf{V}_{k,s}^{x[i]} \mathbf{H}$ and $\mathbf{H}^\top \mathbf{V}_{k,s}^{x[i]} \mathbf{y}_{k,s}^{[i]}$ as innovation part related to \mathbf{x}_k).

(2) Time Update Step (Prediction)

After the n_k batch of measurements is processed sequentially, performing (20) and (21) to accomplish the prediction step.

$$\hat{\mathbf{q}}_{k+1}^{x[0]} = \mathbf{\Omega}_{k+1}^{x[0]} \mathbf{F}_k^x \mathbf{\Omega}_k^{x[n_k]}^{-1} \hat{\mathbf{q}}_k^{x[n_k]} \quad (20a)$$

$$\mathbf{\Omega}_{k+1}^{x[0]} = \mathbf{W}_w^x - \mathbf{W}_w^x \mathbf{F}_k^x \left(\mathbf{\Omega}_k^{x[n_k]} + \mathbf{F}_k^{x\top} \mathbf{W}_w^x \mathbf{F}_k^x \right)^{-1} \mathbf{F}_k^{x\top} \mathbf{W}_w^x \quad (20b)$$

$$\hat{\mathbf{q}}_{k+1}^{p[0]} = \mathbf{\Omega}_{k+1}^{p[0]} \mathbf{F}_k^p \left(\mathbf{\Omega}_k^{p[n_k]} \right)^{-1} \hat{\mathbf{q}}_k^{p[n_k]} \quad (21a)$$

$$\mathbf{\Omega}_{k+1}^{p[0]} = \mathbf{W}_w^p - \mathbf{W}_w^p \mathbf{F}_k^p \left(\mathbf{\Omega}_k^{p[n_k]} + \mathbf{F}_k^{p\top} \mathbf{W}_w^p \mathbf{F}_k^p \right)^{-1} \mathbf{F}_k^{p\top} \mathbf{W}_w^p. \quad (21b)$$

The detailed CEOT filter is collected in Algorithm 1.

Algorithm 1: Centralized EOT (CEOT) Filter

```

1 Initialization:  $\hat{\mathbf{x}}_1^{[0]}$ ,  $\hat{\mathbf{p}}_1^{[0]}$ ,  $\mathbf{\Omega}_1^{x[0]}$ , and  $\mathbf{\Omega}_1^{p[0]}$ ;
2 for  $k \leftarrow 1, 2, \dots$  // scan time do
3   Data:  $\{\mathbf{y}_{k,s}^i\}_{i=1}^{n_k}$  ( $s \in \mathcal{N}$ );
4   Initialization:  $\hat{\mathbf{x}}_k^{[0]}$ ,  $\hat{\mathbf{p}}_k^{[0]}$ ,  $\mathbf{\Omega}_k^{x[0]}$ , and  $\mathbf{\Omega}_k^{p[0]}$ ;
5   for  $i = 1, 2, \dots, n_k$  // sequential do
6     | compute  $\hat{\mathbf{x}}_k^{[i]}$ ,  $\mathbf{\Omega}_k^{x[i]}$ ,  $\hat{\mathbf{p}}_k^{[i]}$ ,  $\mathbf{\Omega}_k^{p[i]}$  via (18) and (19)
7   end for
8   Output1:  $\hat{\mathbf{x}}_k \leftarrow \left( \mathbf{\Omega}_k^{x[n_k]} \right)^{-1} \hat{\mathbf{q}}_k^{x[n_k]}$ ,  $\mathbf{C}_k^x \leftarrow \left( \mathbf{\Omega}_k^{x[n_k]} \right)^{-1}$ ;
9   Output2:  $\hat{\mathbf{p}}_k \leftarrow \left( \mathbf{\Omega}_k^{p[n_k]} \right)^{-1} \hat{\mathbf{q}}_k^{p[n_k]}$ ,  $\mathbf{C}_k^p \leftarrow \left( \mathbf{\Omega}_k^{p[n_k]} \right)^{-1}$ ;
10  Prediction: compute  $\hat{\mathbf{q}}_{k+1}^{x[0]}$ ,  $\mathbf{\Omega}_{k+1}^{x[0]}$ ,  $\hat{\mathbf{q}}_{k+1}^{p[0]}$ ,  $\mathbf{\Omega}_{k+1}^{p[0]}$  via (20) and (21)
11 end for

```

Notice that using (6) and (13) to achieve the corresponding filters poses that the cross-correlation between \mathbf{x}_k and \mathbf{p}_k exists in the $[i]$ -th and $[i-1]$ -th sequential operation. Here, we just take CEOT filter as an example to show the cross-correlation (see Fig. 2).

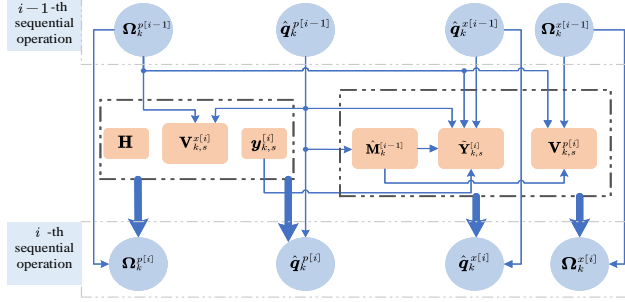


Figure 2: An illustration of the cross-correlation between \mathbf{x}_k and \mathbf{p}_k .

5. Distributed Extended Object Tracking Filters

Indeed, the centralized tracking system gathers the accumulated measurements $\mathcal{Y}_k = \{\mathcal{Y}_{k,s}\}_{s \in \mathcal{S}}$ to provide an optimal estimate. However, the distributed fusion system has some appealing advantages over the centralized system for overcoming the communication bandwidth constraints, single-node failure, and congestion of massive data. This section aims to extend the models (6) and (13) to make them feasible in a realistic distributed scenario. To this end, we apply two schemes, namely consensus on information and consensus on measurement, to achieve consensus estimates among all nodes, respectively. Considering the existence of multiple measurements on sensor nodes, before yielding the final results, the sequential processing technique is used at each time step.

5.1. Distributed Consensus on Information Filter

Since communication nodes \mathcal{C} do not have observations about EO, their local estimates are often erroneous. Error covariance is an indicator to point out the error range of estimates. Hence, a reasonable solution is that the estimate in a local node is appropriately weighted by its information matrix. Then a node with less information about the estimated state will have less weight in the consensus process [28, 29]. Inspired by the idea, we propose a distributed CI information filter, where each local node sends the information vector and information matrix to its neighboring nodes (i.e., track-to-track fusion).

Next, we first define a convex combination (CC) fusion rule. Then, we will show how to incorporate the rule into CI filter.

Definition 1 (Convex Combination fusion). Assume the sensor network \mathcal{N} is strongly connected and undirected, given the consensus weights $\{\pi^{s,j}\}$ (e.g., the Metropolis weights [30]) satisfying $\pi^{s,j} \geq 0$ and $\sum_{j \in \mathcal{N}^s} \pi^{s,j} = 1, \forall s, j \in \mathcal{N}$ to ensure that the consensus matrix $\mathbf{\Pi}$ is primitive and doubly stochastic¹, one has $\lim_{l \rightarrow \infty} \pi_l^{s,j} = \frac{1}{|\mathcal{N}|}$ [31]. Here, $\pi^{s,j}$ is the (s, j) -th entry of the matrix $\mathbf{\Pi}$, $\pi_l^{s,j}$ denotes the (s, j) -th entry of $\mathbf{\Pi}^l$, and $|\mathcal{N}|$ is the cardinality of \mathcal{N} . Then, for a state set $\{\mathbf{x}_s\}_{s \in \mathcal{N}}$, the state \mathbf{x}_s at node s is updated at iteration l as $\mathbf{x}_s(l) = \sum_{j \in \mathcal{N}^s} \pi^{s,j} \mathbf{x}_s(l-1)$ with initialization $\mathbf{x}_s(0) = \mathbf{x}_s$, resulting in $\lim_{l \rightarrow \infty} \mathbf{x}_s(l) = \frac{1}{|\mathcal{N}|} \sum_{s \in \mathcal{N}} \mathbf{x}_s, \forall s \in \mathcal{N}$.

Assume that, at time k , each node $s \in \mathcal{N}$ provides an information set $\{\hat{\mathbf{q}}_{k,s}^{x^{[i]}}, \hat{\mathbf{q}}_{k,s}^{p^{[i]}}, \mathbf{\Omega}_{k,s}^{x^{[i]}}, \mathbf{\Omega}_{k,s}^{p^{[i]}}\}$. Then, at each iteration, each node s calculates a linear combination of quantities in \mathcal{N}^s with suitable weights $\pi^{s,j}, j \in \mathcal{N}^s$ (i.e., using CC fusion). By alternatively doing this between nodes, the iteration operation yields the averages $\sum_{s \in \mathcal{N}} \{\hat{\mathbf{q}}_{k,s}^{x^{[i]}}, \hat{\mathbf{q}}_{k,s}^{p^{[i]}}, \mathbf{\Omega}_{k,s}^{x^{[i]}}, \mathbf{\Omega}_{k,s}^{p^{[i]}}\} / |\mathcal{N}|$ when the number of iterations L approaches to ∞ . Thus, the ultimate outputs are $\hat{\mathbf{x}}_{k,s} = \sum_{s \in \mathcal{N}} (\mathbf{\Omega}_{k,s}^{x^{[n_k]}} \hat{\mathbf{x}}_{k,s}^{x^{[n_k]}}) / \sum_{s \in \mathcal{N}} \mathbf{\Omega}_{k,s}^{x^{[n_k]}}$ and $\hat{\mathbf{p}}_{k,s} = \sum_{s \in \mathcal{N}} (\mathbf{\Omega}_{k,s}^{p^{[n_k]}} \hat{\mathbf{p}}_{k,s}^{p^{[n_k]}}) / \sum_{s \in \mathcal{N}} \mathbf{\Omega}_{k,s}^{p^{[n_k]}}$.

¹A non-negative consensus matrix $\mathbf{\Pi}$ is doubly stochastic if all its rows and columns sum up to 1. Further, it is primitive if there exists an integer l such that all the elements of $\mathbf{\Pi}^l$ are strictly positive [31].

However, to save the computation cost, the maximum iteration L should be a trade-off between cost and performance. CI filter consists of the following three steps:

(1) Measurement Update Step (Correction)

If node $s \in \mathcal{S}$, compute

$$\hat{\mathbf{q}}_{k,s}^{x[i]} = \hat{\mathbf{q}}_{k,s}^{x[i-1]} + \mathbf{H}^\top \mathbf{V}_{k,s}^{-x[i]} \mathbf{y}_{k,s}^i \quad (22a)$$

$$\mathbf{\Omega}_{k,s}^{x[i]} = \mathbf{\Omega}_{k,s}^{x[i-1]} + \mathbf{H}^\top \mathbf{V}_{k,s}^{-x[i]} \mathbf{H} \quad (22b)$$

$$\hat{\mathbf{q}}_{k,s}^{p[i]} = \hat{\mathbf{q}}_{k,s}^{p[i-1]} + \left(\hat{\mathbf{M}}_{k,s}^{[i]} \right)^\top \mathbf{V}_{k,s}^{p[i]} \tilde{\mathbf{Y}}_{k,s}^{[i]} \quad (23a)$$

$$\mathbf{\Omega}_{k,s}^{p[i]} = \mathbf{\Omega}_{k,s}^{p[i-1]} + \left(\hat{\mathbf{M}}_{k,s}^{[i]} \right)^\top \mathbf{V}_{k,s}^{p[i]} \hat{\mathbf{M}}_{k,s}^{[i]}. \quad (23b)$$

If node $s \in \mathcal{C}$, let

$$\hat{\mathbf{q}}_{k,s}^{x[i]} = \hat{\mathbf{q}}_{k,s}^{x[i-1]}, \quad \mathbf{\Omega}_{k,s}^{x[i]} = \mathbf{\Omega}_{k,s}^{x[i-1]} \quad (24a)$$

$$\hat{\mathbf{q}}_{k,s}^{p[i]} = \hat{\mathbf{q}}_{k,s}^{p[i-1]}, \quad \mathbf{\Omega}_{k,s}^{p[i]} = \mathbf{\Omega}_{k,s}^{p[i-1]}. \quad (24b)$$

(2) Consensus Step (Consensus)

Perform CC fusion on $\hat{\mathbf{q}}_{k,s}^{x[i]}$, $\hat{\mathbf{q}}_{k,s}^{p[i]}$, $\mathbf{\Omega}_{k,s}^{x[i]}$, $\mathbf{\Omega}_{k,s}^{p[i]}$ independently for L iterations (L is designed a priori).

(3) Time Update Step (Prediction)

After n_k batch of measurements are processed sequentially, skip (20) and (21) to calculate the predicted information matrices and information vectors on each node $s \in \mathcal{N}$.

The detailed CI filter is shown in Algorithm 2. It is worth noting that CI filter gives a convergent solution even in a single consensus iteration ($L = 1$) [28]. Moreover, the performance of CI filter is less sensitive to more measurements since it directly broadcasts the information quantities to achieve consensus.

5.2. Distributed Consensus on Measurement Filter

Since the temporal evolution models of both the kinematic state and extent are same on each node, the local prediction step will have an identical form as in CEOT filter. Thus, the remaining objective is to compute the summation terms of innovation parts

$$\begin{aligned} \Delta \hat{\mathbf{q}}_k^{x[i]} &:= \sum_{s \in \mathcal{S}} \mathbf{H}^\top \mathbf{V}_{k,s}^{-x[i]} \mathbf{y}_{k,s}^i, \quad \Delta \mathbf{\Omega}_k^{x[i]} := \sum_{s \in \mathcal{S}} \mathbf{H}^\top \mathbf{V}_{k,s}^{-x[i]} \mathbf{H} \\ \Delta \hat{\mathbf{q}}_k^{p[i]} &:= \sum_{s \in \mathcal{S}} \left(\hat{\mathbf{M}}_{k,s}^{[i-1]} \right)^\top \mathbf{V}_{k,s}^{p[i]} \tilde{\mathbf{Y}}_{k,s}^{[i]} \\ \Delta \mathbf{\Omega}_k^{p[i]} &:= \sum_{s \in \mathcal{S}} \left(\hat{\mathbf{M}}_{k,s}^{[i-1]} \right)^\top \mathbf{V}_{k,s}^{p[i]} \hat{\mathbf{M}}_{k,s}^{[i-1]} \end{aligned}$$

in CEOT filter as shown in (18) and (19) via a distributed way [25]. Once the objective is complete, consensus is reached with the assistance of measurement-to-measurement fusion. The effective fusion strategy falls into the CM scope. To this end, each node $s \in \mathcal{N}$ computes a linear combination of innovation parts from its neighboring nodes $j \in \mathcal{N}^s$ to update its values by using CC fusion. The operation yields approximately averaged values on node s (assume the maximum iteration L is a suitable value) when consensus is complete, while CEOT filter needs $\left\{ \Delta \mathbf{\Omega}_k^{p[i]}, \Delta \hat{\mathbf{q}}_k^{p[i]}, \Delta \mathbf{\Omega}_k^{x[i]}, \Delta \hat{\mathbf{q}}_k^{x[i]} \right\}$. This inconsistency is partially compensated by multiplying a suitable weight $\omega_{k,s}^{[i]}$ after consensus iteration. The CM information filter consists of the following four steps:

Algorithm 2: Consensus on Information (CI) Filter

```

1 Initialization:  $\hat{\mathbf{x}}_{1,s}^{[0]}$ ,  $\hat{\mathbf{p}}_{1,s}^{[0]}$ ,  $\mathbf{\Omega}_{1,s}^{x[0]}$ , and  $\mathbf{\Omega}_{1,s}^{p[0]}$ ;
2 for  $k \leftarrow 1, 2, \dots$  // scan time do
3   Data:  $\{\mathbf{y}_{k,s}^i\}_{i=1}^{n_k}$  ( $s \in \mathcal{N}$ );
4   Initialization:  $\hat{\mathbf{x}}_{k,s}^{[0]}$ ,  $\hat{\mathbf{p}}_{k,s}^{[0]}$ ,  $\mathbf{\Omega}_{k,s}^{x[0]}$ , and  $\mathbf{\Omega}_{k,s}^{p[0]}$ ;
5   for  $i = 1, 2, \dots, n_k$  // sequential do
6     Correction;
7     if  $s \in \mathcal{S}$  then
8       | compute  $\hat{\mathbf{q}}_{k,s}^{x[i]}$ ,  $\mathbf{\Omega}_{k,s}^{x[i]}$ ,  $\hat{\mathbf{q}}_{k,s}^{p[i]}$ ,  $\mathbf{\Omega}_{k,s}^{p[i]}$  via (22) and (23)
9     else
10      | compute  $\hat{\mathbf{q}}_{k,s}^{x[i]}$ ,  $\mathbf{\Omega}_{k,s}^{x[i]}$ ,  $\hat{\mathbf{q}}_{k,s}^{p[i]}$ ,  $\mathbf{\Omega}_{k,s}^{p[i]}$  via (24a) and (24b)
11    end if
12    Consensus operation;
13    set  $\hat{\mathbf{q}}_{k,s}^{x[i]}(0) \leftarrow \hat{\mathbf{q}}_{k,s}^{x[i]}$ ,  $\mathbf{\Omega}_{k,s}^{x[i]}(0) \leftarrow \mathbf{\Omega}_{k,s}^{x[i]}$ ,  $\hat{\mathbf{q}}_{k,s}^{p[i]}(0) \leftarrow \hat{\mathbf{q}}_{k,s}^{p[i]}$ ,  $\mathbf{\Omega}_{k,s}^{p[i]}(0) \leftarrow \mathbf{\Omega}_{k,s}^{p[i]}$ ;
14    for  $l = 0, \dots, L-1$  do
15      | perform CC on  $\hat{\mathbf{q}}_{k,s}^{x[i]}$ ,  $\hat{\mathbf{q}}_{k,s}^{p[i]}$ ,  $\mathbf{\Omega}_{k,s}^{x[i]}$ ,  $\mathbf{\Omega}_{k,s}^{p[i]}$ 
16    end for
17    let  $\hat{\mathbf{q}}_{k,s}^{x[i]} \leftarrow \hat{\mathbf{q}}_{k,s}^{x[i]}(L)$ ,  $\mathbf{\Omega}_{k,s}^{x[i]} \leftarrow \mathbf{\Omega}_{k,s}^{x[i]}(L)$ ,  $\hat{\mathbf{q}}_{k,s}^{p[i]} \leftarrow \hat{\mathbf{q}}_{k,s}^{p[i]}(L)$ ,  $\mathbf{\Omega}_{k,s}^{p[i]} \leftarrow \mathbf{\Omega}_{k,s}^{p[i]}(L)$ 
18  end for
19  Output1:  $\hat{\mathbf{x}}_{k,s} \leftarrow \left(\mathbf{\Omega}_{k,s}^{x[n_k]}\right)^{-1} \hat{\mathbf{q}}_{k,s}^{x[n_k]}$ ,  $\mathbf{C}_{k,s}^x \leftarrow \left(\mathbf{\Omega}_{k,s}^{x[n_k]}\right)^{-1}$ ;
20  Output2:  $\hat{\mathbf{p}}_{k,s} \leftarrow \left(\mathbf{\Omega}_{k,s}^{p[n_k]}\right)^{-1} \hat{\mathbf{q}}_{k,s}^{p[n_k]}$ ,  $\mathbf{C}_{k,s}^p \leftarrow \left(\mathbf{\Omega}_{k,s}^{p[n_k]}\right)^{-1}$ ;
21  Prediction: as in Algorithm 1
22 end for

```

(1) Compute local innovation parts

If node $s \in \mathcal{S}$, let

$$\delta \hat{\mathbf{q}}_{k,s}^{x[i]} = \mathbf{H}^\top \mathbf{V}_{k,s}^{x[i]} \mathbf{y}_{k,s}^i, \quad \delta \mathbf{\Omega}_{k,s}^{x[i]} = \mathbf{H}^\top \mathbf{V}_{k,s}^{x[i]} \mathbf{H} \quad (25a)$$

$$\delta \hat{\mathbf{q}}_{k,s}^{p[i]} = \left(\hat{\mathbf{M}}_{k,s}^{[i-1]}\right)^\top \mathbf{V}_{k,s}^{p[i]} \tilde{\mathbf{Y}}_{k,s}^{[i]}, \quad (25b)$$

$$\delta \mathbf{\Omega}_{k,s}^{p[i]} = \left(\hat{\mathbf{M}}_{k,s}^{[i-1]}\right)^\top \mathbf{V}_{k,s}^{p[i]} \hat{\mathbf{M}}_{k,s}^{[i-1]}. \quad (25c)$$

If node $s \in \mathcal{C}$, let

$$\delta \hat{\mathbf{q}}_{k,s}^{x[i]} = \mathbf{0}, \quad \delta \mathbf{\Omega}_{k,s}^{x[i]} = \mathbf{0}, \quad \delta \hat{\mathbf{q}}_{k,s}^{p[i]} = \mathbf{0}, \quad \delta \mathbf{\Omega}_{k,s}^{p[i]} = \mathbf{0}. \quad (26)$$

(2) Consensus Step (Consensus)

Perform CC fusion on $\delta \mathbf{\Omega}_{k,s}^{x[i]}$, $\delta \hat{\mathbf{q}}_{k,s}^{x[i]}$, $\delta \mathbf{\Omega}_{k,s}^{p[i]}$, $\delta \hat{\mathbf{q}}_{k,s}^{p[i]}$ independently for L iterations (L is designed a priori).

(3) Measurement Update Step (Correction)

$$\hat{\mathbf{q}}_{k,s}^{x[i]} = \hat{\mathbf{q}}_{k,s}^{x[i-1]} + \omega_{k,s}^{[i]} \delta \hat{\mathbf{q}}_{k,s}^{x[i]}(L) \quad (27a)$$

$$\mathbf{\Omega}_{k,s}^{x[i]} = \mathbf{\Omega}_{k,s}^{x[i-1]} + \omega_{k,s}^{[i]} \delta \mathbf{\Omega}_{k,s}^{x[i]}(L) \quad (27b)$$

$$\hat{\mathbf{q}}_{k,s}^{p[i]} = \hat{\mathbf{q}}_{k,s}^{p[i-1]} + \omega_{k,s}^{[i]} \delta \hat{\mathbf{q}}_{k,s}^{p[i]}(L) \quad (28a)$$

$$\mathbf{\Omega}_{k,s}^{p[i]} = \mathbf{\Omega}_{k,s}^{p[i-1]} + \omega_{k,s}^{[i]} \delta \mathbf{\Omega}_{k,s}^{p[i]}(L). \quad (28b)$$

(4) Time Update Step (Prediction)

The prediction step is the same as shown in CI filter.

The equations (27) and (28) imply that only the innovation parts are exchanged between nodes while the local priors are neglected in CM filter, which causes its performance being sensitive to the number of measurements (a detailed discussion is shown in section 6.1). Therefore, its convergence more depends on the number of iterations to ensure sufficient innovation interaction when the number of measurements is given. The detailed CM filter is summarized in Algorithm 3.

Algorithm 3: Consensus on Measurement (CM) Filter

```

1 Initialization:  $\hat{\mathbf{x}}_{1,s}^{[0]}, \hat{\mathbf{p}}_{1,s}^{[0]}, \mathbf{\Omega}_{1,s}^{x[0]}$ , and  $\mathbf{\Omega}_{1,s}^{p[0]}$ ;
2 for  $k \leftarrow 1, 2, \dots$  // scan time do
3   Data:  $\{\mathbf{y}_{k,s}^i\}_{i=1}^{n_k}$  ( $s \in \mathcal{N}$ );
4   Initialization:  $\hat{\mathbf{x}}_{k,s}^{[0]}, \hat{\mathbf{p}}_{k,s}^{[0]}, \mathbf{\Omega}_{k,s}^{x[0]}$ , and  $\mathbf{\Omega}_{k,s}^{p[0]}$ ;
5   for  $i = 1, 2, \dots, n_k$  // sequential do
6     Compute local innovation parts;
7     if  $s \in \mathcal{S}$  then
8       | compute  $\delta \hat{\mathbf{q}}_{k,s}^{x[i]}, \delta \mathbf{\Omega}_{k,s}^{x[i]}, \delta \hat{\mathbf{q}}_{k,s}^{p[i]}, \delta \mathbf{\Omega}_{k,s}^{p[i]}$  via (25a) and (25b)
9     else
10      | compute  $\delta \hat{\mathbf{q}}_{k,s}^{x[i]}, \delta \mathbf{\Omega}_{k,s}^{x[i]}, \delta \hat{\mathbf{q}}_{k,s}^{p[i]}, \delta \mathbf{\Omega}_{k,s}^{p[i]}$  via (26)
11    end if
12    Consensus operation;
13    set  $\delta \hat{\mathbf{x}}_{k,s}^{[i]}(0) \leftarrow \delta \hat{\mathbf{x}}_{k,s}^{[i]}$ ,  $\delta \mathbf{\Omega}_{k,s}^{x[i]}(0) \leftarrow \delta \mathbf{\Omega}_{k,s}^{x[i]}$ ,  $\delta \hat{\mathbf{p}}_{k,s}^{[i]}(0) \leftarrow \delta \hat{\mathbf{p}}_{k,s}^{[i]}$ ,  $\delta \mathbf{\Omega}_{k,s}^{p[i]}(0) \leftarrow \delta \mathbf{\Omega}_{k,s}^{p[i]}$ ;
14    for  $l = 0, \dots, L-1$  do
15      | perform CC on  $\delta \hat{\mathbf{x}}_{k,s}^{[i]}, \delta \mathbf{\Omega}_{k,s}^{x[i]}, \delta \hat{\mathbf{p}}_{k,s}^{[i]}, \delta \mathbf{\Omega}_{k,s}^{p[i]}$ 
16    end for
17    Correction;
18    compute  $\hat{\mathbf{q}}_{k,s}^{x[i]}, \mathbf{\Omega}_{k,s}^{x[i]}, \hat{\mathbf{q}}_{k,s}^{p[i]}, \mathbf{\Omega}_{k,s}^{p[i]}$  via (27) and (28)
19  end for
20  Output1:  $\hat{\mathbf{x}}_{k,s} = \left(\mathbf{\Omega}_{k,s}^{x[n_k]}\right)^{-1} \hat{\mathbf{q}}_{k,s}^{x[n_k]}$ ,  $\mathbf{C}_{k,s}^x = \left(\mathbf{\Omega}_{k,s}^{x[n_k]}\right)^{-1}$ ;
21  Output2:  $\hat{\mathbf{p}}_{k,s} = \left(\mathbf{\Omega}_{k,s}^{p[n_k]}\right)^{-1} \hat{\mathbf{q}}_{k,s}^{p[n_k]}$ ,  $\mathbf{C}_{k,s}^p = \left(\mathbf{\Omega}_{k,s}^{p[n_k]}\right)^{-1}$ ;
22  Prediction: as in Algorithm 1
23 end for

```

6. Simulation Examples

To the best of our knowledge, the existing distributed EOT filters have not been explored the network $(\mathcal{S}, \mathcal{C}, \mathcal{A})$ used in the paper. Hence, we evaluate the performance of the proposed CEOT, CI, and CM in a simple dynamic scenario and compare them with a centralized approach based on the RM model [19]. We assess both the position and extent errors by the Gaussian Wasserstein distance as described in [7, 32]. Meanwhile, a novel metric, the Averaged consensus estimate error (ACEE), is used to testify the estimate

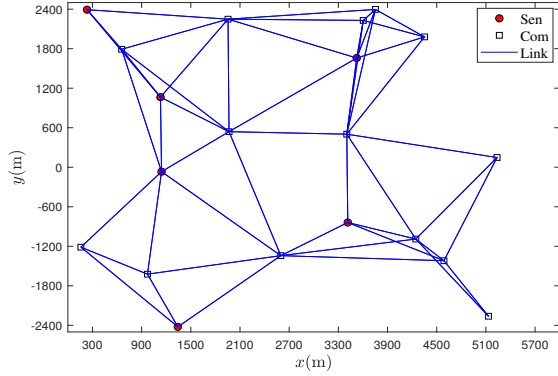


Figure 3: Sensor network with maximum communication distance $R = 2000\text{m}$.

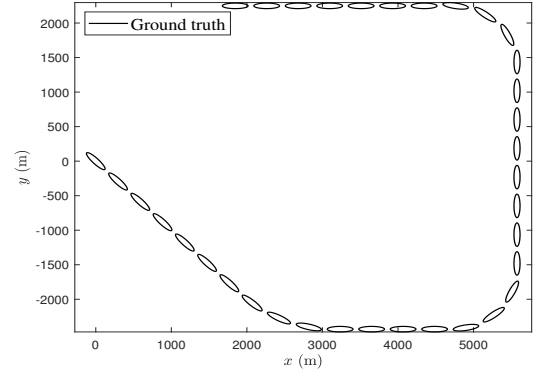


Figure 4: Trajectory of an elliptical extended object.

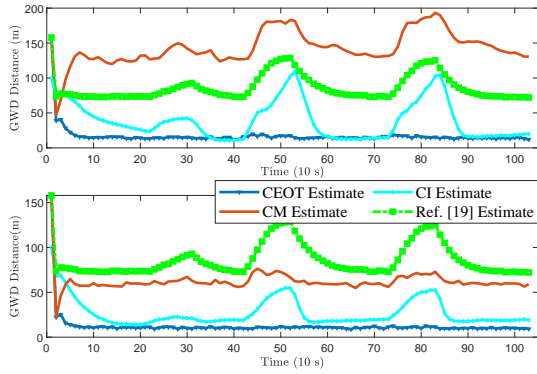


Figure 5: Simulation with iteration $L = 6$. The first row shows the GWDs of different filters with $\lambda = 5$. The second row shows the GWDs of different filters with $\lambda = 10$.

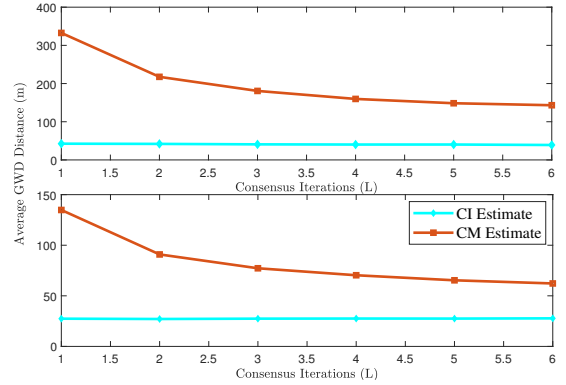


Figure 6: Simulation with different consensus iterations. The first row shows the Average GWDs of different filters with $\lambda = 5$. The second row shows the Average GWDs of different filters with $\lambda = 10$.

bias between different nodes.

$$\text{ACEE} := \frac{1}{|\mathcal{N}|(|\mathcal{N}| - 1)} \sum_{s \in \mathcal{N}} \sum_{j \in \mathcal{N}} \|\hat{\mathbf{x}}_k^s - \hat{\mathbf{x}}_k^j\|$$

where $\hat{\mathbf{x}}_k^s$ is the estimate at node s .

The network consists of 14 communication nodes and 6 sensor nodes as shown in Fig 3. The consensus parameter $\pi^{s,j}$ is computed by the Metropolis weights rule [33]. As for the scalar weights $\omega_{k,s}$, one can refer to [25, eq. (4)].

6.1. Ellipse with Nearly Constant Velocity Model Scenario

In this scenario, the extended object is an ellipse with lengths of the semi-axes 170m and 40m. The object moves with nearly constant speed $v = 50\text{km/h}$ following the trajectory as shown in Fig. 4. The parameters used in the examined filters are listed in Table 1.

The comparison results focus on the GWD for comparing ellipses and the ACEE metric over $M = 100$ Monte Carlo runs. Moreover, comparison in the simulated scenario allows an in-depth analysis of the proposed filters as the performance is varied under different conditions.

Table 1: Tracker Parameter Settings

Parameters	Specification
Scan Time	$T = 10$ s
Measurement Noise Cov.	$\mathbf{C}_s^v = \text{diag}(200, 8)$
Multiplicative Noise Cov.	$\mathbf{C}_s^h = \frac{1}{4}\mathbf{I}_2$
Process Noise Cov. w.r.t Kine.	$\mathbf{C}_w^x = \text{diag}(50, 50, 1, 1)$
Process Noise Cov. w.r.t Extent	$\mathbf{C}_w^p = \text{diag}(0.05, 1, 1)$
Kine. vector	$\hat{\mathbf{x}}_{1,s}^{[0]} = [100, 100, 10, -17]^\top$
Exten. vector	$\hat{\mathbf{p}}_{1,s}^{[0]} = [-\pi/3, 200, 90]^\top$
Cov. matrix w.r.t Kine.	$\mathbf{C}_{1,s}^{x[0]} = \text{diag}(900, 900, 16, 16)$
Cov. matrix w.r.t Extent	$\mathbf{C}_{1,s}^{p[0]} = \text{diag}(0.2, 400, 400)$
Kine. transition matrix	$\mathbf{F}_k^s = \begin{bmatrix} 1 & 0 & T & 0 \\ 0 & 1 & 0 & T \\ 0 & 0 & 1 & 0 \\ 0 & 0 & 0 & 1 \end{bmatrix}$
Extent transition matrix	$\mathbf{F}_k^p = \mathbf{I}_3$
Degrees of freedom used in [19]	$\alpha_{0 0} = 10$
Agility constant used in [19]	$\tau = 50$

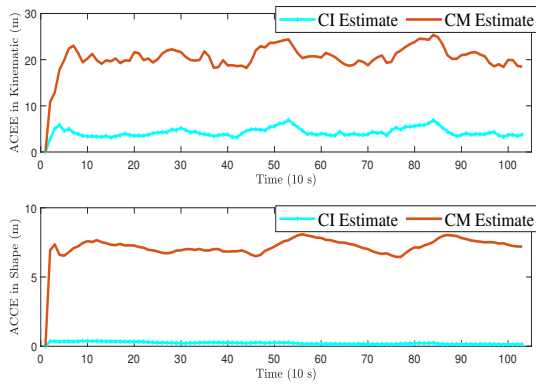


Figure 7: ACEEs of different filters with iteration $L = 6$ and $\lambda = 5$.

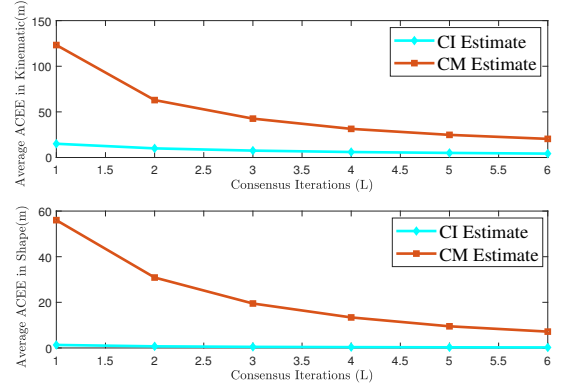


Figure 8: ACEEs of different filters with different consensus iterations under $\lambda = 5$.

Fig. 5 shows the GWDs for the examined filters. For the two distributed filters, CI has a lower GWD error than that of CM in this scenario. A reason is that CM directly broadcasts local innovation parts to its neighboring nodes, while CI exchanges the information quantities (including the local priors and innovation parts). Hence, CM will depend more on the number of measurements, especially in the EOT realm with multiple measurements per scan time. Fig. 5 verifies the conclusion by comparing the GWDs in two cases (i.e., the number of measurements follows a Poisson distribution with means $\lambda = 5$ and $\lambda = 10$). The other reason is that CI provides a stable solution even by a single consensus iteration, but CM needs infinite iterations to ensure consensus weights the $\pi^{s,j} \rightarrow \frac{1}{|\mathcal{N}|}$. Then, CM converges to CEOT with $\omega_{k,s} = |\mathcal{N}|$. However, the number of iterations should be selected as a trade-off between computation burden and performance. Here, we set the consensus iterations $L = 6$ to yield a converged output, and simultaneously cause an inconsistency between CEOT and CM.

CEOT gathering all of the measurements from sensor nodes gives a benchmark. With CEOT, the uncertainty of the semi-axes lengths is modeled by a low process noise, and the orientation is described by a high process noise. In contrast, the approach-based RM model [19] uses a single constant τ to denote the extent evolution over time, resulting in a larger GWD error.

It is worth noting that the GWDs in CM have a decreased tendency with more iterations and measurements (see Figs. 5-6). In contrast, CI has reached a stable value at the first iteration and is less sensitive to more measurements. Hence, according to the theoretical analysis and simulation results, a reasonable anticipation is that as the number of iterations and measurements increases, CM will obtain better results.

Fig. 7 shows that the differences between different nodes for the kinematics and extent estimate are within a reasonable range. These results demonstrate the validity of the proposed filters adopting the corresponding consensus strategies. With increasing consensus iterations, better consensus (lower ACEE) on local estimates is achieved as shown in Fig. 8. Again, CM still has a decreased tendency with more iterations while CI almost tends to a stable value during the previous iterations.

7. Conclusion

This paper proposes the centralized and distributed extended object tracking information filters based on a nonlinear and state-coupled model. To this end, we first separate the model into two linear models without losing the cross-correlation between the estimated states. To make the centralized information filter available in computation, we convert the measurements into a summation form of innovation parts. The two distributed information filters are derived by exchange the information quantities and measurements between neighboring nodes, respectively. Numerical results testify the consistency and convergence of the proposed filters in different parameters. Combined with the numerical results and theoretical analysis, one can anticipate the proposed filters are applicable on the other types of sensor networks [34].

Further developments are devoted to investigating extensions of the pseudo-linearized measurement models, e.g., secure state estimation under sensor attacks [35, 36], state estimation over heterogeneous sensor networks [37, 38], state estimation under multiple constraints [39, 40], and distributed event-triggered system [41, 42].

Acknowledgment

This work is supported by the National Natural Science Foundation of China (Grant no. 61873205 and 61771399).

Appendix A

PROOF OF PROPOSITION 2. It is shown that (11) does not exist a direct mapping between the extent \mathbf{p}_k and pseudo-measurement $\mathbf{Y}_{k,s}^{[i]}$. To extract the term \mathbf{p}_k from (11), substituting (3) and (9) into (11) yields

(A.1),

$$\mathbf{Y}_{k,s}^{[i]} \approx \mathbf{F} \left(\left(\mathbf{H}\mathbf{x}_k - \mathbf{H}\hat{\mathbf{x}}_k^{[i-1]} + \hat{\mathbf{S}}_k^{[i-1]} \mathbf{h}_{k,s}^{[i]} + \begin{bmatrix} \left(\mathbf{h}_{k,s}^{[i]} \right)^\top \hat{\mathbf{J}}_{1,k}^{[i-1]} \\ \left(\mathbf{h}_{k,s}^{[i]} \right)^\top \hat{\mathbf{J}}_{2,k}^{[i-1]} \end{bmatrix} \left(\mathbf{p}_k - \hat{\mathbf{p}}_k^{[i-1]} \right) + \mathbf{v}_{k,s}^{[i]} \right) \otimes (\cdot) \right) \quad (\text{A.1a})$$

$$:= [Y_1^2 \ Y_2^2 \ Y_1 Y_2]^\top, \quad (\text{A.1b})$$

where the notation (\cdot) denotes the term right before it. Now, our goal becomes to construct an equivalent measurement model $\mathbf{Y}_{k,s}^{[i]} \approx \mathbf{H}_k^p \mathbf{p}_k + \mathbf{v}_{k,s}^{p[i]}$ about \mathbf{p}_k from (A.1a), where \mathbf{H}_k^p is the measurement matrix and $\mathbf{v}_{k,s}^{p[i]}$ the measurement noise. Meanwhile, its first and second moment need to equal to the expectation and covariance of (11) as much as possible. We first define $\mathbf{H}\mathbf{x}_k - \mathbf{H}\hat{\mathbf{x}}_k^{[i-1]} := [\tilde{x}_1 \ \tilde{x}_2]^\top$, $\mathbf{H}\mathbf{C}_k^{x[i-1]}\mathbf{H}^\top := \begin{bmatrix} c_{11}^x & c_{12}^x \\ c_{21}^x & c_{22}^x \end{bmatrix}$, $\mathbf{C}_{k,s}^{y[i]} := \begin{bmatrix} c_{11}^y & c_{12}^y \\ c_{21}^y & c_{22}^y \end{bmatrix}$, $\hat{\mathbf{S}}_k^{[i-1]} := [\hat{\mathbf{S}}_1^\top \ \hat{\mathbf{S}}_2^\top]^\top$, $\mathbf{v}_{k,s}^{[i]} := [v_1 \ v_2]^\top$, $\text{Cov}(\mathbf{v}_{k,s}^{[i]}) := \text{diag} \begin{bmatrix} \sigma_1^2 & 0 \\ 0 & \sigma_2^2 \end{bmatrix}$ and omit the superscript $[\cdot]$, time index k , and sensor node index s . Then, we further expand (A.1b) as follows

$$\begin{aligned} Y_1^2 &= \tilde{x}_1^2 + (\hat{\mathbf{S}}_1 \mathbf{h})^\top (\cdot) + \left(\mathbf{h}^\top \hat{\mathbf{J}}_1 (\mathbf{p} - \hat{\mathbf{p}}) \right)^\top (\cdot) + v_1^2 + 2\tilde{x}_1 \hat{\mathbf{S}}_1 \mathbf{h} + 2\tilde{x}_1 \mathbf{h}^\top \hat{\mathbf{J}}_1 (\mathbf{p} - \hat{\mathbf{p}}) + 2\tilde{x}_1 v_1 + 2\hat{\mathbf{S}}_1 \mathbf{h} \mathbf{h}^\top \hat{\mathbf{J}}_1 (\mathbf{p} - \hat{\mathbf{p}}) \\ &\quad + 2\hat{\mathbf{S}}_1 \mathbf{h} v_1 + 2\mathbf{h}^\top \hat{\mathbf{J}}_1 (\mathbf{p} - \hat{\mathbf{p}}) v_1 - 2\hat{\mathbf{S}}_1 \mathbf{C}^h \hat{\mathbf{J}}_1 \mathbf{p} + 2\hat{\mathbf{S}}_1 \mathbf{C}^h \hat{\mathbf{J}}_1 \mathbf{p} \end{aligned} \quad (\text{A.2a})$$

$$\begin{aligned} Y_2^2 &= \tilde{x}_2^2 + (\hat{\mathbf{S}}_2 \mathbf{h})^\top (\cdot) + \left(\mathbf{h}^\top \hat{\mathbf{J}}_2 (\mathbf{p} - \hat{\mathbf{p}}) \right)^\top (\cdot) + v_2^2 + 2\tilde{x}_2 \hat{\mathbf{S}}_2 \mathbf{h} + 2\tilde{x}_2 \mathbf{h}^\top \hat{\mathbf{J}}_2 (\mathbf{p} - \hat{\mathbf{p}}) + 2\tilde{x}_2 v_2 + 2\hat{\mathbf{S}}_2 \mathbf{h} \mathbf{h}^\top \hat{\mathbf{J}}_2 (\mathbf{p} - \hat{\mathbf{p}}) \\ &\quad + 2\hat{\mathbf{S}}_2 \mathbf{h} v_2 + 2\mathbf{h}^\top \hat{\mathbf{J}}_2 (\mathbf{p} - \hat{\mathbf{p}}) v_2 - 2\hat{\mathbf{S}}_2 \mathbf{C}^h \hat{\mathbf{J}}_2 \mathbf{p} + 2\hat{\mathbf{S}}_2 \mathbf{C}^h \hat{\mathbf{J}}_2 \mathbf{p} \end{aligned} \quad (\text{A.2b})$$

$$\begin{aligned} Y_1 Y_2 &= \tilde{x}_1 \tilde{x}_2 + (\hat{\mathbf{S}}_1 \mathbf{h})^\top (\hat{\mathbf{S}}_2 \mathbf{h}) + \left(\mathbf{h}^\top \hat{\mathbf{J}}_1 (\mathbf{p} - \hat{\mathbf{p}}) \right)^\top \left(\mathbf{h}^\top \hat{\mathbf{J}}_2 (\mathbf{p} - \hat{\mathbf{p}}) \right) + v_1 v_2 + 2\tilde{x}_1 \hat{\mathbf{S}}_2 \mathbf{h} + 2\tilde{x}_1 \mathbf{h}^\top \hat{\mathbf{J}}_2 (\mathbf{p} - \hat{\mathbf{p}}) + 2\tilde{x}_1 v_2 \\ &\quad + 2\hat{\mathbf{S}}_1 \mathbf{h} \mathbf{h}^\top \hat{\mathbf{J}}_2 (\mathbf{p} - \hat{\mathbf{p}}) + 2\hat{\mathbf{S}}_1 \mathbf{h} v_2 + 2\mathbf{h}^\top \hat{\mathbf{J}}_1 (\mathbf{p} - \hat{\mathbf{p}}) v_2 + \hat{\mathbf{S}}_2 \mathbf{C}^h \hat{\mathbf{J}}_1 \mathbf{p} + \hat{\mathbf{S}}_1 \mathbf{C}^h \hat{\mathbf{J}}_2 \mathbf{p} - \hat{\mathbf{S}}_2 \mathbf{C}^h \hat{\mathbf{J}}_1 \mathbf{p} - \hat{\mathbf{S}}_1 \mathbf{C}^h \hat{\mathbf{J}}_2 \mathbf{p}. \end{aligned} \quad (\text{A.2c})$$

The expectation of (A.2) is given as follows:

$$\mathbb{E}(Y_1^2) = c_{11}^x + \hat{\mathbf{S}}_1 \mathbf{C}^h \hat{\mathbf{S}}_1^\top + \text{tr}(\mathbf{C}^p \hat{\mathbf{J}}_1^\top \mathbf{C}^h \hat{\mathbf{J}}_1) + \sigma_1^2 - 2\hat{\mathbf{S}}_1 \mathbf{C}^h \hat{\mathbf{J}}_1 \mathbf{p} + 2\hat{\mathbf{S}}_1 \mathbf{C}^h \hat{\mathbf{J}}_1 \mathbf{p} \quad (\text{A.3a})$$

$$\mathbb{E}(Y_2^2) = c_{22}^x + \hat{\mathbf{S}}_2 \mathbf{C}^h \hat{\mathbf{S}}_2^\top + \text{tr}(\mathbf{C}^p \hat{\mathbf{J}}_2^\top \mathbf{C}^h \hat{\mathbf{J}}_2) + \sigma_2^2 - 2\hat{\mathbf{S}}_2 \mathbf{C}^h \hat{\mathbf{J}}_2 \mathbf{p} + 2\hat{\mathbf{S}}_2 \mathbf{C}^h \hat{\mathbf{J}}_2 \mathbf{p} \quad (\text{A.3b})$$

$$\mathbb{E}(Y_1 Y_2) = c_{12}^x + \hat{\mathbf{S}}_1 \mathbf{C}^h \hat{\mathbf{S}}_2^\top + \text{tr}(\mathbf{C}^p \hat{\mathbf{J}}_1^\top \mathbf{C}^h \hat{\mathbf{J}}_2) + \hat{\mathbf{S}}_2 \mathbf{C}^h \hat{\mathbf{J}}_1 \mathbf{p} + \hat{\mathbf{S}}_1 \mathbf{C}^h \hat{\mathbf{J}}_2 \mathbf{p} - \hat{\mathbf{S}}_2 \mathbf{C}^h \hat{\mathbf{J}}_1 \mathbf{p} - \hat{\mathbf{S}}_1 \mathbf{C}^h \hat{\mathbf{J}}_2 \mathbf{p}. \quad (\text{A.3c})$$

The equation (A.2a) implies $\mathbb{E}(Y_1) = \mathbb{E}(Y_2) = 0$, $\text{Cov}(Y_1) = c_{11}^y$, $\text{Cov}(Y_1 Y_2) = c_{12}^y$ and $\text{Cov}(Y_2) = c_{22}^y$. From Wick's theorem [43], we get

$$\begin{cases} \mathbb{E}\{(Y_1^2)^2\} = 3(c_{11}^y)^2, \mathbb{E}\{(Y_2^2)^2\} = 3(c_{22}^y)^2, \mathbb{E}\{Y_1^3 Y_2\} = 3(c_{11}^y c_{12}^y) \\ \mathbb{E}\{Y_1 Y_2^3\} = 3(c_{22}^y c_{12}^y), \mathbb{E}\{(Y_1^2 Y_2^2)\} = c_{11}^y c_{22}^y + 2(c_{12}^y)^2 \end{cases}. \quad (\text{A.4})$$

By rearranging (A.2b), (A.3), and (A.4) yields

$$\begin{bmatrix} Y_1^2 \\ Y_2^2 \\ Y_1 Y_2 \end{bmatrix} = \hat{\mathbf{M}} \mathbf{p} + \mathbf{v}^p \quad (\text{A.5})$$

with expectation $\mathbf{F}\text{vect}(\mathbf{C}^y)$ and covariance $\mathbf{F}(\mathbf{C}^y \otimes \mathbf{C}^y)(\mathbf{F} + \tilde{\mathbf{F}})^\top$. Then, we have the measurement model as shown in (13), and find the measurement matrix $\mathbf{H}^p = \hat{\mathbf{M}}$. These two moments of (A.5) equal to the expectation and covariance of (11), respectively, which means that (A.5) achieves the moment matching. In fact, for the last few terms of (A.2), other terms can be chosen to make the equation hold. Choosing those terms in $\hat{\mathbf{M}}$ ensures (11) and (A.1a) giving an identical result on computing the cross-covariance between \mathbf{Y} and \mathbf{p} , while choosing other terms cannot satisfy this condition. Until now, the proof is complete.

References

- [1] K. Granström, M. Baum, S. Reuter, Extended object tracking: Introduction, overview, and applications, *J. Adv. Inf. Fusion* 12 (2017) 139–174.
- [2] J. W. Koch, Bayesian approach to extended object and cluster tracking using random matrices, *IEEE Trans. Aerosp. Electron. Syst.* 44 (3) (2008) 1042–1059. doi:10.1109/TAES.2008.4655362.
- [3] J. Lan, X. R. Li, Tracking of extended object or target group using random matrix: new model and approach, *IEEE Trans. Aerosp. Electron. Syst.* 52 (6) (2016) 2973–2989. doi:10.1109/TAES.2016.130346.
- [4] X. Cao, J. Lan, X. R. Li, Y. Liu, Extended object tracking using automotive radar, in: *Proc. 2018 21st Int. Conf. Inf. Fusion*, Cambridge, UK, 2018, pp. 1–5. doi:10.23919/ICIF.2018.8455293.
- [5] K. Granström, J. Bramstång, Bayesian smoothing for the extended object random matrix model, *IEEE Trans. Signal Process.* 67 (14) (2019) 3732–3742. doi:10.1109/TSP.2019.2920471.
- [6] J. Lan, X. R. Li, Extended-object or group-target tracking using random matrix with nonlinear measurements, *IEEE Trans. Signal Process.* 67 (19) (2019) 5130–5142. doi:10.1109/TSP.2019.2935866.
- [7] S. Yang, M. Baum, Extended kalman filter for extended object tracking, in: *Proc. 2017 IEEE Int. Conf. Acoust., Speech and Signal Process. (ICASSP)*, New Orleans, LA, USA, 2017, pp. 4386–4390. doi:10.1109/ICASSP.2017.7952985.
- [8] S. Yang, M. Baum, Tracking the orientation and axes lengths of an elliptical extended object, *IEEE Trans. Signal Process.* 67 (18) (2019) 4720–4729. doi:10.1109/TSP.2019.2929462.
- [9] M. Baum, U. D. Hanebeck, Shape tracking of extended objects and group targets with star-convex rhms, in: *Proc. 14th Int. Conf. Inf. Fusion*, 2011, pp. 1–8.
- [10] M. Kumru, E. Özkan, 3d extended object tracking using recursive gaussian processes, in: *Proc. 2018 21st Int. Conf. Inf. Fusion*, Cambridge, UK, 2018, pp. 1–8. doi:10.23919/ICIF.2018.8455480.
- [11] W. Aftab, R. Hostettler, A. D. Freitas, M. Arvaneh, L. Mihaylova, Spatio-temporal gaussian process models for extended and group object tracking with irregular shapes, *IEEE Trans. Veh. Technol.* 68 (3) (2019) 2137–2151. doi:10.1109/TVT.2019.2891006.
- [12] S. Lee, J. McBride, Extended object tracking via positive and negative information fusion, *IEEE Trans. Signal Process.* 67 (7) (2019) 1812–1823. doi:10.1109/TSP.2019.2897942.
- [13] H. Kaulbersch, J. Honer, M. Baum, A cartesian b-spline vehicle model for extended object tracking, in: *Proc. 2018 21st Int. Conf. Inf. Fusion*, Cambridge, UK, 2018, pp. 1–5. doi:10.23919/ICIF.2018.8455717.
- [14] A. Zea, F. Faion, M. Baum, U. D. Hanebeck, Level-set random hypersurface models for tracking nonconvex extended objects, *IEEE Trans. Aerosp. Electron. Syst.* 52 (6) (2016) 2990–3007. doi:10.1109/TAES.2016.130704.
- [15] Y. Liang, X. Dong, H. Wang, L. Han, Q. Li, Z. Ren, Distributed finite time cubature information filtering with unknown correlated measurement noises, *ISA Trans.* 112 (2021) 35–55. doi:https://doi.org/10.1016/j.isatra.2020.12.011.
- [16] L. Yan, C. Di, Q. M. J. Wu, Y. Xia, S. Liu, Distributed fusion estimation for multisensor systems with non-gaussian but heavy-tailed noises, *ISA Trans.* 101 (2020) 160–169. doi:https://doi.org/10.1016/j.isatra.2020.02.004.
- [17] G. Xiao, . Liu, Distributed fault-tolerant model predictive control for intermittent fault: A cooperative way, *ISA Trans.* 89 (2019) 113–121. doi:https://doi.org/10.1016/j.isatra.2018.12.022.
- [18] G. Vivone, K. Granström, P. Braca, P. Willett, Multiple sensor bayesian extended target tracking fusion approaches using random matrices, in: *Proc. 2016 19th Int. Conf. Inf. Fusion*, Heidelberg, Germany, 2016, pp. 886–892.
- [19] G. Vivone, P. Braca, K. Granström, P. Willett, Multistatic bayesian extended target tracking, *IEEE Trans. Aerosp. Electron. Syst.* 52 (6) (2016) 2626–2643. doi:10.1109/TAES.2016.150724.
- [20] W. Li, Y. Jia, D. Meng, J. Du, Distributed tracking of extended targets using random matrices, in: *Proc. 2015 54th IEEE Conf. on Decision and Control (CDC)*, Osaka, Japan, 2015, pp. 3044–3049. doi:10.1109/CDC.2015.7402676.
- [21] J. Liu, G. Guo, Distributed asynchronous extended target tracking using random matrix, *IEEE Sensors Journal* 20 (2) (2020) 947–956. doi:10.1109/JSEN.2019.2944280.
- [22] J. Hua, C. Li, Distributed variational bayesian algorithms for extended object tracking, *arXiv Preprint*: 1903.00182.
- [23] C. Liang, F. Wen, Z. Wang, Trust-based distributed kalman filtering for target tracking under malicious cyber attacks, *Inf. Fusion* 46 (7) (2019) 44–50. doi:10.1016/j.inffus.2018.04.002.
- [24] J. Hua, C. Li, Distributed variational bayesian algorithms over sensor networks, *IEEE Trans. Signal Process.* 64 (3) (2016) 783–798. doi:10.1109/TSP.2015.2493979.
- [25] G. Battistelli, L. Chisci, G. Mugnai, A. Farina, A. Graziano, Consensus-based linear and nonlinear filtering, *IEEE Trans. Autom. Control* 60 (5) (2015) 1410–1415. doi:10.1109/TAC.2014.2357135.
- [26] Y. Bar-Shalom, X. R. Li, T. Kirubarajan, Estimation with applications to tracking and navigation: theory algorithms and software, John Wiley & Sons, Inc., 2004.
- [27] M. Baum, F. Faion, , U. D. Hanebeck, Modeling the target extent with multiplicative noise, in: *Proc. 15th Int. Conf. Inf. Fusion*, Singapore, Singapore, 2012, pp. 2406–2412.

- [28] G. Battistelli, L. Chisci, Stability of consensus extended kalman filter for distributed state estimation, *Automatica* 68 (2016) 169–178. doi:<https://doi.org/10.1016/j.automatica.2016.01.071>.
- [29] G. Battistelli, L. Chisci, , C. Fantacci, Parallel consensus on likelihoods and priors for networked nonlinear filtering, *IEEE Signal Process. Lett.* 21 (7) (2014) 787–791. doi:[10.1109/LSP.2014.2316258](https://doi.org/10.1109/LSP.2014.2316258).
- [30] G. Battistelli, L. Chisci, Stability of consensus extended kalman filtering for distributed state estimation, *IFAC Proceedings Volumes* 47 (3) (2014) 5520–5525. doi:<https://doi.org/10.3182/20140824-6-ZA-1003.01993>.
- [31] G. Battistelli, L. Chisci, Kullback–leibler average, consensus on probability densities, and distributed state estimation with guaranteed stability, *Automatica* 50 (3) (2014) 707–718. doi:<https://doi.org/10.1016/j.automatica.2013.11.042>.
- [32] S. Yang, M. Baum, Second-order extended kalman filter for extended object and group tracking, in: *Proc. 2016 19th Int. Conf. Inf. Fusion, Heidelberg, Germany, 2016*, pp. 1178–1184.
- [33] W. Li, G. Wei, F. Han, Y. Liu, Weighted average consensus-based unscented kalman filtering, *IEEE Trans. Cybern.* 46 (2) (2016) 558–567. doi:[10.1109/TCYB.2015.2409373](https://doi.org/10.1109/TCYB.2015.2409373).
- [34] A. T. Kamal, J. A. Farrell, A. K. Roy-Chowdhury, Information weighted consensus filters and their application in distributed camera networks, *IEEE Trans. Autom. Control* 58 (12) (2013) 3112–3125. doi:[10.1109/TAC.2013.2277621](https://doi.org/10.1109/TAC.2013.2277621).
- [35] Y. Guan, X. Ge, Distributed attack detection and secure estimation of networked cyber-physical systems against false data injection attacks and jamming attacks, *IEEE Trans. Signal Inf. Process. Netw.* 4 (1) (2018) 48–59. doi:[10.1109/TSIPN.2017.2749959](https://doi.org/10.1109/TSIPN.2017.2749959).
- [36] W. Ao, Y. Song, C. Wen, Distributed secure state estimation and control for cps under sensor attacks, *IEEE Trans. Cybern.* 50 (1) (2020) 259–269. doi:[10.1109/TCYB.2018.2868781](https://doi.org/10.1109/TCYB.2018.2868781).
- [37] Z. She, Q. Hao, Q. Liang, L. Wang, Invariant set based distributed protocol for synchronization of discrete-time heterogeneous systems with nonlinear dynamics, *ISA Trans.* 102 (2020) 56–67. doi:<https://doi.org/10.1016/j.isatra.2019.07.023>.
- [38] H. Mahboubi, K. Moezzi, A. G. Aghdam, K. Sayrafian-Pour, Distributed sensor coordination algorithms for efficient coverage in a network of heterogeneous mobile sensors, *IEEE Trans. Autom. Control* 62 (11) (2017) 5954–5961. doi:[10.1109/TAC.2017.2714102](https://doi.org/10.1109/TAC.2017.2714102).
- [39] T. Wang, J. Qiu, H. Gao, Adaptive neural control of stochastic nonlinear time-delay systems with multiple constraints, *IEEE Trans. Syst., Man, Cybern., Syst.* 47 (8) (2017) 1875–1883. doi:[10.1109/TSMC.2016.2562511](https://doi.org/10.1109/TSMC.2016.2562511).
- [40] L. D. *et al*, Adaptive neural network-based tracking control for full-state constrained wheeled mobile robotic system, *IEEE Trans. Syst., Man, Cybern., Syst.* 47 (8) (2017) 2410–2419. doi:[10.1109/TSMC.2017.2677472](https://doi.org/10.1109/TSMC.2017.2677472).
- [41] T. Li, H. Zhao, Y. Chang, A novel event-triggered communication strategy for second-order multiagent systems, *ISA Trans.* 97 (2020) 93–101. doi:<https://doi.org/10.1016/j.isatra.2019.07.022>.
- [42] J. Sun, T. Long, Event-triggered distributed zero-sum differential game for nonlinear multi-agent systems using adaptive dynamic programming, *ISA Trans.* 110 (2021) 39–52. doi:<https://doi.org/10.1016/j.isatra.2020.10.043>.
- [43] G. Wick, The evaluation of the collision matrix, *Phys. Rev.* 80 (2) (1950) 268–272. doi:[10.1103/PhysRev.80.268](https://doi.org/10.1103/PhysRev.80.268).